Performance-Aware Quantizer Synthesis for LQI Tracking Subject to Fixed Level Budgets

Mircea Șușcă[1], *Member, IEEE*, Vlad Mihaly[1], *Member, IEEE*, Vineeth Satheeskumar Varma[2,1], and Irinel-Constantin Morărescu[2,1]

***Abstract*— We study finite-level static measurement quantizers for discrete-time linear-quadratic-integral (LQI) tracking (servo) problems. In several practical cases, the hardware imposes a fixed communication-rate (quantization budget) constraint. In this setup, for the augmented LQI loop with quantized state and output measurements, we prove an ℓ_∞–input-to-state stability (ISS) bound with respect to bounded reference inputs and bounded component-wise quantization errors. Furthermore, to ensure a well-posed performance criterion under practical stability, we introduce a discounted control-law distortion index measuring deviation from the nominal (unquantized) LQI command. We then derive an explicit upper bound that links this discounted distortion to a weighted sum-of-squared quantization errors, with constant sensitivity weights computed offline from the nominal closed-loop design. Under a component-wise scalar architecture, the resulting data-driven synthesis reduces to weighted 1D quantizer design problems and a finite level-allocation problem, both solved globally by dynamic programming. Simulations show that the proposed scheme outperforms uniform, logarithmic, and Lloyd-Max designs.**

***Index Terms*— quantization; dynamic programming; input-to-state stability; LQI control; discounted quadratic cost**

I. Introduction

Quantization is ubiquitous in cyber-physical systems, arising from finite-precision hardware and bandwidth-limited sensing. Quantizer synthesis is well-studied in signal processing, including distributed filtering [1], [2], edge inference [3], and goal-oriented communication [4], but these designs are typically open-loop. In feedback control, quantization alters the closed-loop dynamics and can affect stability and performance, motivating foundational work on quantized stabilization and networked control under information constraints [5], [6]. However, many control approaches rely on adaptive/zooming mechanisms or redesign the controller around a prescribed quantizer [7]–[9]; fewer provide constructive, performance-driven synthesis of static finite-level measurement quantizers.

We focus on distributed and networked implementations in which the sensing side is resource-constrained, whereas the actuation side is comparatively less constrained. Consequently, it is natural to target the measurement channels for quantizer synthesis. We consider an LQI (servo) architecture because it provides a unified linear-quadratic framework for both stabilization and reference tracking [10], [11], used in a wide range of applications, many of which operate in distributed control environments [12]. From a quantized networked control standpoint, this generality is important: trajectory distributions and operating regions are reference-dependent, which directly impacts how measurement quantizers should allocate resolution. Furthermore, in many applications domains, the reference is prescribed *a priori*, either as programmed setpoint profiles, e.g., ramp-soak thermal recipes, or as planned motion trajectories in robotics [13]. As such, quantizer synthesis can leverage the expected operating regions induced by that known reference.

Related works address quantization in control under different objectives, including quantized actuation in optimal control [14], data-driven control with denial-of-service and quantized measurements [15], privacy-oriented stochastic quantization [16], and data-rate versus performance tradeoffs in networked control [17]. In contrast, we synthesize static finite-level measurement quantizers under optimally allocated per-channel level budgets, explicitly aligned with LQI performance.

This letter proposes an end-to-end framework that bridges quantized stability analysis with a constructive quantizer synthesis procedure accounting for the LQI performance criterion. Our contribution is three-fold: (*i*) establish a tailored ISS-type practical stability guarantee for the quantized LQI closed-loop under a no-saturation condition, accommodating non-uniform finite-level quantization; (*ii*) derive a discounted command-distortion upper-bound of the deviation of the implemented control input from the ideal LQI command by a weighted quadratic function of the quantization errors; (*iii*) specialize to a product (component-wise) architecture which yields independent weighted 1D data-driven subproblems and a finite level-allocation problem, both globally solved by dynamic programming under a fixed total level budget.

The remainder of the letter is organized as follows. Section II presents the problem statement. Section III establishes practical stability in an ℓ_∞–ISS sense for arbitrary feasible vector quantizers. Section IV develops the globally optimizable surrogate criterion and resulting dynamic programming synthesis procedure. Section V illustrates the method on a representative case study. Section VI concludes and outlines future directions.

Notations: Let $\mathbb{Z}_{\geq 0}$ be the set of non-negative integers. For

This work was supported by project DECIDE, no. 57/14.11.2022 funded under the PNRR I8 scheme by the Romanian Ministry of Research, Innovation, and Digitisation.

[1] Automation Department, Technical University of Cluj-Napoca, 400114, Cluj-Napoca, Romania (e-mails: {mircea.susca, vlad.mihaly, vineeth.varma, constantin.morarescu}@aut.utcluj.ro).

[2] Université de Lorraine, CNRS, CRAN, 54000 Nancy, France.(e-mails: {vineeth.satheeskumar-varma, constantin.morarescu}@univ-lorraine.fr).

column vectors $v \in \mathbb{R}^d$ and matrices $X \in \mathbb{R}^{d\times d}$, we denote their ∞-norms as $\|v\|_\infty$ and $\|X\|_\infty$, along with their Euclidean norms as $\|v\|_2$ and $\|X\|_2$. We denote $X_1 (\succeq) \succ X_2$ if $X_1 - X_2$ is (semi-)positive definite. For a bounded sequence $\{v_k\}_{k\geq 0}$, we write $\|v\|_{\ell_\infty} := \sup_{k\geq 0} \|v_k\|_\infty$. The ℓ-th component of $x_k = (x_{k,1}, \dots, x_{k,n})^\top \in \mathbb{R}^n$ is denoted by $x_{k,\ell}$.

II. Problem Statement

We consider a discrete-time linear time-invariant (LTI) process under LQI control, as in Figure 1. Its dynamics, along with augmented integrator states are:

$$x_{k+1} = Ax_k + Bu_k,\ y_k = Cx_k, \quad x_0 \in \mathbb{R}^n,\ k \in \mathbb{Z}_{\geq 0}, \tag{1}$$

$$z_{k+1} = z_k + \tau\,(r_k - y_k^q), \quad z_0 \in \mathbb{R}^p, \tag{2}$$

where $x_k \in \mathbb{R}^n$, $u_k \in \mathbb{R}^m$, $y_k \in \mathbb{R}^p$, $z_k \in \mathbb{R}^p$. Furthermore, $r_k \in \mathbb{R}^p$ is an exogenous reference and $\tau > 0$ is a fixed sampling period. State (2) is the integrated error term computed using the forward Euler discretization of $\dot{z}(t) = r(t) - y(t)$.

Remark 1: Alternative architectures quantize the tracking error: $z_{k+1} = z_k + \tau\, q_e(r_k - y_k)$. All subsequent results can be recast by rewriting (2) as $z_{k+1} = z_k + \tau(r_k - y_k) + \tau\, e_{e,k}$ with additional bounded disturbance $e_{e,k} := q_e(r_k - y_k) - (r_k - y_k)$.

The controller receives only quantized measurements:

$$x_k^q := \mathbf{q}_x(x_k), \quad y_k^q := \mathbf{q}_y(y_k), \tag{3}$$

where $\mathbf{q}_x : \mathbb{R}^n \to \mathcal{Q}_x \subset \mathbb{R}^n$ and $\mathbf{q}_y : \mathbb{R}^p \to \mathcal{Q}_y \subset \mathbb{R}^p$ are static finite-level (possibly non-uniform) *vector* quantizers. The quantizer operating ranges are prescribed (by hardware) as:

$$\mathcal{X} := \{x \in \mathbb{R}^n :\ |x_i| \leq X_i,\ i = \overline{1,n}\}, \tag{4a}$$

$$\mathcal{Y} := \{y \in \mathbb{R}^p :\ |y_j| \leq Y_j,\ j = \overline{1,p}\}, \tag{4b}$$

and inputs outside $\mathcal{X}$ or $\mathcal{Y}$ are interpreted as saturated.

We define the quantization errors:

$$e_{x,k} := x_k^q - x_k, \quad e_{y,k} := y_k^q - y_k. \tag{5}$$

When no saturation occurs, each quantizer admits known per-coordinate error envelopes $\bar{e}_x \in \mathbb{R}^n_{\geq 0}$, $\bar{e}_y \in \mathbb{R}^p_{\geq 0}$ such that:

$$|e_{x,k}| \leq \bar{e}_x, \quad |e_{y,k}| \leq \bar{e}_y. \tag{6}$$

In particular, $\|e_{x,k}\|_\infty \leq \|\bar{e}_x\|_\infty$ and $\|e_{y,k}\|_\infty \leq \|\bar{e}_y\|_\infty$. The quantizers will be further detailed in Sections III and IV.

The LQI control law uses quantized state feedback and the integral state, according to Figure 1:

$$u_k = K_x x_k^q + K_z z_k, \tag{7}$$

and we assume ideal actuation channels, with no quantization or transmission error. This setup models scenarios where sensing and telemetry is bandwidth-limited (e.g., wireless sensor networks or remote monitoring), so that measurements

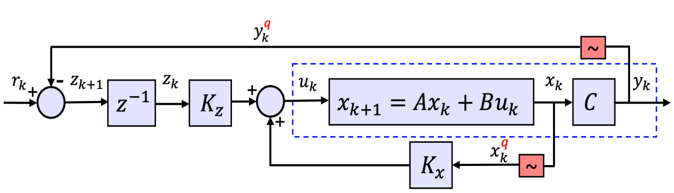

Fig. 1. Quantized LQI tracking control structure

must be compressed (quantized) before transmission, while the actuator link is reliable, by comparison. Accordingly, our quantizer synthesis targets the measurement channels to minimize degradation of the closed-loop LQI performance.

Let the augmented state be defined as $\xi_k := (x_k^\top\ \ z_k^\top)^\top$. Substituting (7) into (1)–(2) yields the closed-loop dynamics:

$$\xi_{k+1} = A_{\mathrm{cl}}\xi_k + Er_k + G_x e_{x,k} + G_y e_{y,k}, \tag{8a}$$

$$A_{\mathrm{cl}} = \begin{pmatrix} A + BK_x & BK_z \\ -\tau C & I \end{pmatrix}, \quad E = \begin{pmatrix} 0 \\ \tau I \end{pmatrix}, \tag{8b}$$

$$G_x = \big((BK_x)^\top \quad 0\big)^\top, \qquad G_y = \big(0 \quad (-\tau I)^\top\big)^\top. \tag{8c}$$

We make the following assumptions.

Assumption 1: In the ideal case $e_{x,k} \equiv 0$, $e_{y,k} \equiv 0$, the gains (K_x, K_z) are obtained from the assumed stabilizing Riccati solution for the infinite-horizon LQI index:

$$J_{\mathrm{LQI}}(\xi_0) := \textstyle\sum_{k=0}^{\infty} \left(\xi_k^\top Q\, \xi_k + u_k^\top R\, u_k\right), \tag{9}$$

using weighting matrices $Q = Q^\top \succeq 0$ and $R = R^\top \succ 0$. Consequently, the resulting matrix A_{cl} is Schur and there exist constants $c > 0$ and $\lambda \in (0, 1)$ such that:

$$\|A_{\mathrm{cl}}^k\|_\infty \leq c\,\lambda^k, \quad \forall k \in \mathbb{Z}_{\geq 0}. \tag{10}$$

Assumption 2: The reference is bounded, i.e., there exists $\bar{r} \in \mathbb{R}^p_{\geq 0}$ such that $|r_k| \leq \bar{r}$, $k \geq 0$; hence $\|r\|_{\ell_\infty} \leq \|\bar{r}\|_\infty$.

The letter focuses on solving the following problem.

Problem 1: Under Assumptions 1 and 2, synthesize static finite-level measurement quantizers $\mathbf{q}_x, \mathbf{q}_y$ under a fixed total level budget for the LQI closed-loop (8) over a prescribed operating set with the goal of reducing performance degradation relative to the nominal unquantized LQI loop.

A quantizer is *feasible* if its domains $\mathcal{X}, \mathcal{Y}$ are non-saturating on the operating set, so that (6) holds along the closed-loop trajectories. Section III provides this certificate and the resulting ISS-type stability bound. Given certified ranges, a fixed total level budget, and nominal unquantized LQI data $\mathcal{D} = \{(x_t^\star, y_t^\star, k_t)\}_{t=1}^M$, Section IV designs component-wise scalar quantizers by allocating levels across channels and choosing their thresholds and reproduction values to globally minimize a data-driven surrogate of this degradation.

III. ISS of the Quantized LQI System

This section first provides a certificate for choosing the quantizer domains $\mathcal{X}$ and $\mathcal{Y}$ from (4) so that no saturation occurs on a prescribed operating set. For quantizers satisfying this certificate, the closed-loop system (8) is a stable linear system driven by bounded inputs, which yields the ISS estimate used in Section IV for performance-oriented quantizer synthesis.

Let $H_x := (I_n\ \ 0)$ and $H_y := (C\ \ 0)$, so that $x_k = H_x \xi_k$ and $y_k = H_y \xi_k$. Fix an initial operating set $\Xi_0 := \{\xi \in \mathbb{R}^{n+p} : |\xi| \leq \bar{\xi}_0\}$, where absolute values and inequalities are component-wise. For $H \in \{H_x, H_y\}$, define:

$$\beta_H := \sup_{k\geq 0} |HA_{\mathrm{cl}}^k|\bar{\xi}_0, \quad \Gamma_H^r := \textstyle\sum_{k=0}^{\infty} |HA_{\mathrm{cl}}^k E|, \tag{11a}$$

$$\Gamma_H^x := \textstyle\sum_{k=0}^{\infty} |HA_{\mathrm{cl}}^k G_x|, \quad \Gamma_H^y := \textstyle\sum_{k=0}^{\infty} |HA_{\mathrm{cl}}^k G_y|. \tag{11b}$$

The above quantities are finite because A_{cl} is Schur.

We separate range certification from performance design. Lemma 1 first certifies $\mathcal{X}, \mathcal{Y}$ for prescribed error envelopes

$\bar{e}_x, \bar{e}_y$. Section IV then places the finite quantization levels and centroids inside the certified domains. The resulting quantizers are required to satisfy the prescribed envelopes; otherwise, the certificate is rechecked with the resulting maximum cell errors.

Lemma 1: Consider system (8a) under Assumptions 1 and 2, with bounds (6) holding whenever the quantizer inputs lie in $\mathcal{X}, \mathcal{Y}$. Let $X = (X_1, \dots, X_n)^\top$ and $Y = (Y_1, \dots, Y_p)^\top$ denote the half-range vectors in (4). If the following component-wise inequalities hold:

$$X \geq \beta_{H_x} + \Gamma^r_{H_x}\bar{r} + \Gamma^x_{H_x}\bar{e}_x + \Gamma^y_{H_x}\bar{e}_y, \qquad (12a)$$

$$Y \geq \beta_{H_y} + \Gamma^r_{H_y}\bar{r} + \Gamma^x_{H_y}\bar{e}_x + \Gamma^y_{H_y}\bar{e}_y, \qquad (12b)$$

then, for every $\xi_0 \in \Xi_0$, the trajectories satisfy $x_k \in \mathcal{X}$ and $y_k \in \mathcal{Y}$ for all $k \geq 0$. Hence, no saturation occurs and the error envelopes above are valid along the closed-loop trajectories.

Proof: For the base case, since $A^0_{\mathrm{cl}} = I$, $\xi_0 \in \Xi_0$ gives $|H\xi_0| \leq \beta_H$ for $H \in \{H_x, H_y\}$; hence (12) implies $|x_0| \leq X$, $|y_0| \leq Y$, i.e., $x_0 \in \mathcal{X}$, $y_0 \in \mathcal{Y}$.

Assume, by contradiction, that a first exit time $k^\star \geq 1$ exists. Then, $\forall\, t < k^\star$, the quantizers are unsaturated and the bounds $|e_{x,t}| \leq \bar{e}_x$, $|e_{y,t}| \leq \bar{e}_y$ hold. Iterating (8a) leads to:

$$\xi_k = A^k_{\mathrm{cl}}\xi_0 + \textstyle\sum_{t=0}^{k-1} A^{k-1-t}_{\mathrm{cl}}(Er_t + G_x e_{x,t} + G_y e_{y,t}). \qquad (13)$$

At $k = k^\star$, pre-multiplying by $H \in \{H_x, H_y\}$ and taking component-wise absolute values gives:

$$|H\xi_{k^\star}| \leq \beta_H + \Gamma^r_H\bar{r} + \Gamma^x_H\bar{e}_x + \Gamma^y_H\bar{e}_y.$$

Using (12) component-wise with $H = H_x$ and $H = H_y$ gives $|x_{k^\star}| \leq X$ and $|y_{k^\star}| \leq Y$, i.e., $x_{k^\star} \in \mathcal{X}$ and $y_{k^\star} \in \mathcal{Y}$, contradicting the first-exit definition. Therefore no such time exists. ■

Theorem 1: Consider the quantized LQI closed-loop (8a) under Assumptions 1 and 2. If the quantizer ranges satisfy (12) in Lemma 1, then (8) is ℓ_∞-ISS with respect to (r, e_x, e_y). In particular, for all $k \in \mathbb{Z}_{\geq 0}$, the following bound holds:

$$\begin{aligned}\|\xi_k\|_\infty \leq c\,\lambda^k\|\xi_0\|_\infty + \frac{c}{1-\lambda}\big(\|E\|_\infty\|\bar{r}\|_\infty + \|G_x\|_\infty\|\bar{e}_x\|_\infty \\ + \|G_y\|_\infty\|\bar{e}_y\|_\infty\big),\end{aligned} \qquad (14)$$

where $c > 0$ and $\lambda \in (0,1)$ are given by (10).

Proof: Iterating (8a) leads to (13). Taking $\|\cdot\|_\infty$, using (10), applying $\|r_k\|_\infty \leq \|\bar{r}\|_\infty$ from Assumption 2, using Lemma 1 to ensure that (6) holds for all k, gives:

$$\begin{aligned}\|\xi_k\|_\infty \leq c\lambda^k\|\xi_0\|_\infty + c\textstyle\sum_{t=0}^{k-1}\lambda^{k-1-t}(\|E\|_\infty\|\bar{r}\|_\infty \\ + \|G_x\|_\infty\|\bar{e}_x\|_\infty + \|G_y\|_\infty\|\bar{e}_y\|_\infty).\end{aligned} \qquad (15)$$

Since $\sum_{t=0}^{k-1}\lambda^{k-1-t} \leq \frac{1}{1-\lambda}$, the bound (14) follows, which guarantees an ℓ_∞-ISS estimate with respect to (r, e_x, e_y). ■

IV. Optimal Quantizer Design

This section proposes the synthesis of static measurement quantizers $\mathbf{q}_x(\cdot)$ and $\mathbf{q}_y(\cdot)$ from (3) under certified ranges and a fixed total level budget, with the goal of minimizing the *control-law distortion* relative to (9) induced by quantization. In view of Theorem 1, any feasible quantizer preserves practical stability. Hence, we now focus on performance. To synthesize the quantizers, we consider a data-driven approach, by collecting a representative set of the ideal closed-loop trajectories.

The setup is to compare the quantized implementation (8) to the ideal (unquantized) LQI loop driven by the *same* reference sequence $\{r_k\}$. The ideal closed-loop satisfies:

$$\xi^\star_{k+1} = A_{\mathrm{cl}}\xi^\star_k + Er_k, \quad u^\star_k := K\,\xi^\star_k = \begin{pmatrix}K_x & K_z\end{pmatrix}\cdot\xi^\star_k. \qquad (16)$$

The quantized implementation can be rewritten as:

$$\xi_{k+1} = A_{\mathrm{cl}}\xi_k + Er_k + \eta_k,$$
$$\eta_k := G_x e_{x,k} + G_y e_{y,k}, \quad u_k = K\xi_k + K_x e_{x,k},$$

with errors (5) satisfying (6) for feasible quantizers. We define the distortion variables $\delta\xi_k := \xi_k - \xi^\star_k$ and $\delta u_k := u_k - u^\star_k$ which lead to the following reference-free deviation dynamics:

$$\delta\xi_{k+1} = A_{\mathrm{cl}}\delta\xi_k + \eta_k, \;\; \delta\xi_0 = 0, \qquad (17a)$$

$$\delta u_k = K\,\delta\xi_k + K_x e_{x,k}. \qquad (17b)$$

Hence, state quantization affects the command u_k directly via $K_x e_{x,k}$, whereas output quantization affects it indirectly through $\delta\xi_k$. Since practical stability allows ξ_k (and thus δu_k) to converge only to a neighborhood, we adopt a *discounted* [18] control-law distortion objective:

$$J_\gamma(\xi_0; \mathbf{q}_x, \mathbf{q}_y) := \textstyle\sum_{k=0}^{\infty}\gamma^k\left(\delta\xi_k^\top Q_\delta\,\delta\xi_k + \delta u_k^\top R\,\delta u_k\right), \qquad (18)$$

with design weights $\gamma \in (0,1)$ and $Q_\delta = Q_\delta^\top \succ 0$, typically chosen as $Q_\delta = Q + \rho I$ with an arbitrarily small $\rho > 0$. A command-dominant variant is obtained by taking $Q_\delta = \rho I$. The quantity (18) is the target discounted degradation. Directly optimizing it over finite-level quantizers is difficult; the next result provides a tractable upper bound used for synthesis. This reflects the networked-control goal of keeping the implemented command u_k and trajectory ξ_k close to their nominal counterparts $u^\star_k$ and $\xi^\star_k$.

Define $\overline{Q} := Q_\delta + K^\top RK \succ 0$ and $\overline{S}$ the unique solution of the discounted Lyapunov equation:

$$\overline{S} = \overline{Q} + \gamma A_{\mathrm{cl}}^\top\overline{S}A_{\mathrm{cl}} \succ 0, \;\; \gamma \in (0,1). \qquad (19)$$

The following result allows us to upper-bound the discounted command-distortion cost (18) by a weighted quadratic function of the quantization errors.

Theorem 2: Consider (17) with $\gamma \in (0,1)$ and suppose A_{cl} is Schur, due to Assumption 1. Then, for any $\varepsilon \in (0,1)$ there exists $\kappa_\varepsilon > 0$ (depending only on ε and on the fixed closed-loop data $A_{\mathrm{cl}}, G_x, G_y, K, R, Q_\delta, \overline{S}, \gamma$) such that, along the closed-loop trajectory generated by any feasible quantizers,

$$J_\gamma(\xi_0; \mathbf{q}_x, \mathbf{q}_y) \leq \kappa_\varepsilon\sum_{k=0}^{\infty}\gamma^k\left(e_{x,k}^\top W_x e_{x,k} + e_{y,k}^\top W_y e_{y,k}\right), \qquad (20)$$

where the (constant) sensitivity weights are:

$$W_x := G_x^\top\overline{S}G_x + K_x^\top RK_x, \quad W_y := G_y^\top\overline{S}G_y. \qquad (21)$$

Proof: From (17b) and the weighted Young inequality $(a+b)^\top R(a+b) \leq (1+\varepsilon)a^\top Ra + \left(1+\frac{1}{\varepsilon}\right)b^\top Rb$, $\varepsilon \in (0,1)$, with $a = K\delta\xi_k$ and $b = K_x e_{x,k}$, we obtain:

$$\delta u_k^\top R\delta u_k \leq (1+\varepsilon)\delta\xi_k^\top K^\top RK\,\delta\xi_k + \left(1+\tfrac{1}{\varepsilon}\right)e_{x,k}^\top K_x^\top RK_x\,e_{x,k}.$$

As such, using $\overline{Q} = Q_\delta + K^\top RK \succ 0$, we obtain:

$$\begin{aligned}\delta\xi_k^\top Q_\delta\,\delta\xi_k + \delta u_k^\top R\delta u_k &\leq \delta\xi_k^\top\left(Q_\delta + (1+\varepsilon)K^\top RK\right)\delta\xi_k \\ &\quad + \left(1+\tfrac{1}{\varepsilon}\right)e_{x,k}^\top K_x^\top RK_x\,e_{x,k} \\ &\leq (1+\varepsilon)\,\delta\xi_k^\top\overline{Q}\,\delta\xi_k + \left(1+\tfrac{1}{\varepsilon}\right)e_{x,k}^\top K_x^\top RK_x\,e_{x,k}.\end{aligned} \qquad (22)$$

Let $V_k := \delta\xi_k^\top \overline{S}\delta\xi_k$ be a Lyapunov function candidate, where $\overline{S}$ solves (19). Using (17a), a direct expansion gives:

$$\gamma V_{k+1} - V_k = -\delta\xi_k^\top \overline{Q}\delta\xi_k + 2\gamma\,\delta\xi_k^\top A_{\mathrm{cl}}^\top \overline{S}\eta_k + \gamma\,\eta_k^\top \overline{S}\eta_k. \quad (23)$$

Define $\chi := \left\|\overline{S}^{1/2} A_{\mathrm{cl}} \overline{Q}^{-1/2}\right\|_2^2$ and $c_\eta := 2\gamma(1+2\gamma\chi)$. Applying Young's inequality to the cross term in (23) leads to:

$$2\gamma\,\delta\xi_k^\top A_{\mathrm{cl}}^\top \overline{S}\eta_k \le \tfrac{1}{2}\,\delta\xi_k^\top \overline{Q}\delta\xi_k + 2\gamma^2\chi\,\eta_k^\top \overline{S}\eta_k.$$

Thus, $\frac{1}{2}\,\delta\xi_k^\top \overline{Q}\delta\xi_k \le V_k - \gamma V_{k+1} + (\gamma + 2\gamma^2\chi)\eta_k^\top \overline{S}\eta_k$. Multiplying by γ^k, summing from $k=0$ to N, and employing:

$$\textstyle\sum_{k=0}^{N} \gamma^k (V_k - \gamma V_{k+1}) = V_0 - \gamma^{N+1} V_{N+1} \le V_0,$$

we obtain (since $\delta\xi_0 = 0$, leading to $V_0 = 0$):

$$\textstyle\sum_{k=0}^{\infty} \gamma^k \delta\xi_k^\top \overline{Q}\delta\xi_k \le c_\eta \sum_{k=0}^{\infty} \gamma^k \eta_k^\top \overline{S}\eta_k. \quad (24)$$

Finally, since $\eta_k = G_x e_{x,k} + G_y e_{y,k}$, we have that:

$$\eta_k^\top \overline{S}\eta_k \le 2e_{x,k}^\top G_x^\top \overline{S} G_x e_{x,k} + 2e_{y,k}^\top G_y^\top \overline{S} G_y e_{y,k}. \quad (25)$$

Combining (22), (24), and (25), one admissible constant in (20) is $\kappa_\varepsilon = \max\left\{2(1+\varepsilon)c_\eta,\ 1+\varepsilon^{-1}\right\}$. With W_x and W_y from (21), this proves (20). ∎

Theorem 2 provides the link between the surrogate and the discounted degradation: if $\mathcal{S}_\gamma := \sum_{k=0}^{\infty} \gamma^k (e_{x,k}^\top W_x e_{x,k} + e_{y,k}^\top W_y e_{y,k})$, then $0 \le J_\gamma \le \kappa_\varepsilon \mathcal{S}_\gamma$. As such, for any sequence of feasible quantizers, $\mathcal{S}_\gamma \to 0$ implies $J_\gamma \to 0$. The bound is only sufficient: conservatism enters through the Young inequalities, the separation of $G_x e_x$, $G_y e_y$, the later product-quantizer restriction, and the sampled surrogate used for synthesis.

In principle, one could attempt to design general vector quantizers $\mathbf{q}_x$, $\mathbf{q}_y$ from (3) to minimize the right-hand side of (20). However, globally optimizing a finite-level vector quantizer is combinatorial and suffers from the curse of dimensionality, making even offline global design intractable beyond very small dimensions. Motivated by the measurement-channel structure and by implementability under fixed hardware alphabets, we therefore specialize to a component-wise architecture (product quantization), in which each coordinate is quantized independently. Index all scalar measurement channels by $\ell \in \mathcal{I} := \{1, \dots, n+p\}$ and define the unified scalar signal:

$$s_{\ell,k} := \begin{cases} x_{k,\ell}, & \ell = \overline{1,n}, \\ y_{k,\ell-n}, & \ell = \overline{n+1, n+p}, \end{cases} \qquad s_{\ell,k}^q := q_\ell(s_{\ell,k}),$$

where each $q_\ell : \mathbb{R} \to \mathbb{R}$ is a finite-level scalar quantizer operating on a prescribed range, according to (4), and with level count N_ℓ. We now define an arbitrary 1D quantizer.

Definition 1 (Scalar finite-level quantizer): Fix $\ell \in \mathcal{I}$. An N_ℓ-level scalar quantizer q_ℓ on $[-S_\ell, S_\ell]$ is specified by thresholds $-S_\ell = b_{\ell,0} < b_{\ell,1} < \dots < b_{\ell,N_\ell} = S_\ell$ and reproduction levels (centroids) $\{c_{\ell,i}\}_{i=1}^{N_\ell}$ with $c_{\ell,i} \in [b_{\ell,i-1}, b_{\ell,i})$, and acts by $q_\ell(\sigma) = c_{\ell,i}$ when $\sigma \in [b_{\ell,i-1}, b_{\ell,i})$, with saturation to the extreme levels outside $[-S_\ell, S_\ell]$.

Set $S_i = X_i$ for $i = 1, \dots, n$ and $S_{n+j} = Y_j$ for $j = 1, \dots, p$. For a designed scalar quantizer, define its no-saturation error envelope by $\bar{e}_\ell := \max_{i=1,\dots,N_\ell} \sup_{\sigma \in [b_{\ell,i-1}, b_{\ell,i})} |c_{\ell,i} - \sigma|$. Then, under no saturation, $|s_{\ell,k}^q - s_{\ell,k}| \le \bar{e}_\ell$. Partitioning $\bar{e} = (\bar{e}_1, \dots, \bar{e}_{n+p})^\top$ as $\bar{e} = (\bar{e}_x^\top\ \bar{e}_y^\top)^\top$ gives the envelopes used in Lemma 1.

This restriction to product quantization yields a separable surrogate. For fixed N_ℓ, $\ell \in \mathcal{I}$, the scalar quantizers are obtained from independent weighted 1D problems, each globally solvable by dynamic programming, as follows.

Lemma 2: Assume $\mathbf{q}_x(\cdot)$ and $\mathbf{q}_y(\cdot)$ are implemented component-wise as above, i.e., $s_{\ell,k}^q = q_\ell(s_{\ell,k})$ for $\ell \in \mathcal{I}$ with q_ℓ as in Definition 1. Define the per-coordinate weights:

$$\alpha_{x,i} := [W_x]_{ii} + \textstyle\sum_{\ell \ne i} |[W_x]_{i\ell}|, \quad i = \overline{1,n}, \quad (26a)$$

$$\alpha_{y,j} := [W_y]_{jj} + \textstyle\sum_{\ell \ne j} |[W_y]_{j\ell}|, \quad j = \overline{1,p}, \quad (26b)$$

based on (21). Then, for all k:

$$e_{x,k}^\top W_x e_{x,k} \le \sum_{i=1}^{n} \alpha_{x,i}\, e_{x,k,i}^2; \quad e_{y,k}^\top W_y e_{y,k} \le \sum_{j=1}^{p} \alpha_{y,j}\, e_{y,k,j}^2.$$

Proof: For any symmetric matrix W and vector e, we have $e^\top W e = \sum_i W_{ii} e_i^2 + 2\sum_{i<j} W_{ij} e_i e_j$, and using $2|e_i e_j| \le e_i^2 + e_j^2$, it follows that:

$$\begin{aligned} e^\top W e &\le \textstyle\sum_i W_{ii} e_i^2 + \sum_{i<j} |W_{ij}|(e_i^2 + e_j^2) \\ &= \textstyle\sum_i \left(W_{ii} + \sum_{\ell \ne i} |W_{i\ell}|\right) e_i^2. \end{aligned}$$

Applying this result with $W = W_x$ and $e = e_{x,k}$ leads to $e_{x,k}^\top W_x e_{x,k} \le \sum_{i=1}^{n} \alpha_{x,i} e_{x,k,i}^2$, and similarly for $W = W_y$, $e = e_{y,k}$, concluding the proof. ∎

Given weighted samples $\{(s_{\ell,t}, \omega_t)\}_{t=1}^{M}$ with the discount-consistent choice $\omega_t = \gamma^{k_t} > 0$ when sample t corresponds to time k_t, define the following weights:

$$\alpha_\ell := \begin{cases} \alpha_{x,\ell}, & \ell = \overline{1,n}; \\ \alpha_{y,\ell-n}, & \ell = \overline{n+1, n+p}, \end{cases} \qquad \tilde{\omega}_{\ell,t} := \omega_t\, \alpha_\ell. \quad (27)$$

Corollary 1: The right-hand side of (20) is upper-bounded by a separable sum-of-scalar squared errors. For all $\ell \in \mathcal{I}$, for fixed N_ℓ, consider the weighted 1D quantizer design problems:

$$\min_{q_\ell \in \mathcal{Q}_\ell(N_\ell, S_\ell)} \widehat{\mathcal{J}}_\ell(q_\ell) := \textstyle\sum_{t=1}^{M} \tilde{\omega}_{\ell,t} \left(s_{\ell,t} - q_\ell(s_{\ell,t})\right)^2, \quad (28)$$

where $\mathcal{Q}_\ell(N_\ell, S_\ell)$ denotes the set of N_ℓ-level scalar quantizers on $[-S_\ell, S_\ell]$. Problems (28) admit globally optimal solutions computable by the 1D dynamic program in Algorithm 1.

Proof: Using Lemma 2 into the bound (20) yields an upper bound on $J_\gamma(\xi_0; \mathbf{q}_x, \mathbf{q}_y)$ that is separable across coordinates:

$$J_\gamma \le \kappa_\varepsilon \textstyle\sum_{k=0}^{\infty} \gamma^k \left(\sum_{i=1}^{n} \alpha_{x,i} e_{x,k,i}^2 + \sum_{j=1}^{p} \alpha_{y,j} e_{y,k,j}^2 \right).$$

Replacing the infinite-horizon discounted sums by the weighted objectives (28) gives a computable separable surrogate.

Because the quantizers are component-wise, each term depends only on one scalar quantizer (q_{x_i} or q_{y_j}), so the design splits into independent weighted 1D quantization problems. Each such problem is the weighted 1D squared-error quantization problem, which admits a globally optimal solution by dynamic programming [19] (see Algorithm 1). ∎

In practice, for each channel $\ell \in \mathcal{I}$, we collect samples $\{s_{\ell,t}\}_{t=1}^{M}$ from representative trajectories of the ideal LQI loop (16) over the operating conditions of interest. For sorted scalar samples, the optimal weighted squared-error assignment consists of contiguous segments. Algorithm 1 exploits this property to compute the globally optimal scalar quantizer, with thresholds placed midway between adjacent centroids.

Algorithm 1 Dynamic program for scalar N_ℓ-level quantizer

Require: Samples $\{s_t\}_{t=1}^M$ with $s_t \in [-S_\ell, S_\ell]$, weights $\{\tilde{\omega}_t\}_{t=1}^M$ with $\tilde{\omega}_t > 0$, number of levels N, $1 \le N \le M$

Ensure: Centroids $\{c_i\}_{i=1}^N$ and thresholds $\{b_i\}_{i=0}^N$ on the prescribed range $[-S_\ell, S_\ell]$ which solve (28)

Sort pairs $(s_t, \tilde{\omega}_t)$ by s_t: $s_{(1)} \le \dots \le s_{(M)}$

Set $W(0){=}S(0){=}S_2(0){=}0$ and compute for $t = 1, \dots, M$:

$$W(t) = \sum_{i=1}^{t} \tilde{\omega}_{(i)},\ S(t) = \sum_{i=1}^{t} \tilde{\omega}_{(i)} s_{(i)},\ S_2(t) = \sum_{i=1}^{t} \tilde{\omega}_{(i)} s_{(i)}^2.$$

For any segment $i{:}j$ with $1 \le i \le j \le M$, define its optimal weighted sum-of-squared-errors (SSE) cost:

$$C(i,j) = (S_2(j) - S_2(i{-}1)) - \tfrac{(S(j) - S(i-1))^2}{W(j) - W(i-1)}.$$

Initialize DP: $D(1,j) \leftarrow C(1,j)$ for $j = 1, \dots, M$

for $k = 2$ **to** N **do**

  for $j = k$ **to** M **do**

    $D(k,j) \leftarrow \min_{i \in \{k-1,\dots,j-1\}} \big(D(k{-}1,i) + C(i{+}1,j)\big)$; store argmin $I(k,j)$

  end for

end for

Backtrack from $(k,j) = (N,M)$ using $I(k,j)$ to obtain segment boundaries

Set c_k as the weighted mean of segment k ($c_1 \le \dots \le c_N$); set $b_0 = -S_\ell$, $b_N = S_\ell$, and $b_k = \frac{1}{2}(c_k + c_{k+1})$

Together, thresholds and centroids define q_ℓ as in Definition 1: cell $[b_{\ell,i-1}, b_{\ell,i})$ is mapped to $c_{\ell,i}$, saturating outside $[-S_\ell, S_\ell]$.

Proposition 1: Algorithm 1 has $O(NM^2)$ complexity. The standard monotonicity of the optimal split indices enables divide-and-conquer acceleration to $O(NM \log M)$, without loss of global optimality.

Although α_ℓ only rescales (28) for fixed N_ℓ, it becomes design-relevant when the total level budget is allocated across channels. To complete the synthesis, suppose that a total budget $N_{\text{total}} \ge |\mathcal{I}| N_{\min}$ is prescribed, where $N_{\min} \ge 1$ is a prescribed minimum number of levels per channel. For each channel $\ell \in \mathcal{I}$ and candidate level count $N_\ell = N$, define the optimal scalar surrogate value based on $\widehat{\mathcal{J}}_\ell$ defined in (28):

$$\Phi_\ell(N) := \min_{q_\ell \in \mathcal{Q}_\ell(N, S_\ell)} \widehat{\mathcal{J}}_\ell(q_\ell). \tag{29}$$

Running Algorithm 1 for channel ℓ with N levels gives $\Phi_\ell(N) = D(N,M)$. The level-allocation problem is then:

$$\min_{\{N_\ell \in \mathbb{Z}_{\ge N_{\min}}\}} \sum_{\ell \in \mathcal{I}} \Phi_\ell(N_\ell) \text{ s.t. } \sum_{\ell \in \mathcal{I}} N_\ell = N_{\text{total}}. \tag{30}$$

Let $\Psi_j(b)$ be the minimum cost of allocating an integer budget b to the first j channels, for $b \ge jN_{\min}$.

Proposition 2: Given the cost curves $\{\Phi_\ell(N)\}$, problem (30) is solved globally by the dynamic programming recursion:

$$\Psi_j(b) = \min_{N_{\min} \le N \le b - (j-1)N_{\min}} \{\Psi_{j-1}(b{-}N) + \Phi_j(N)\}, \tag{31}$$

with $\Psi_0(0) = 0$ and $\Psi_0(b) = +\infty$ for $b > 0$. The globally optimal allocation is obtained by backtracking the minimizing choices from $\Psi_{|\mathcal{I}|}(N_{\text{total}})$.

Proof: For a fixed budget $b \in \mathbb{Z}_{\ge 0}$ and first j channels, channel j receives an admissible level count N, and the remaining budget $b - N$ is optimally assigned to the first $j-1$ channels. Since (31) enumerates all admissible integer choices of N, and $\Phi_j(N)$ is the globally optimal scalar-quantizer cost for that choice, Bellman's principle of optimality gives the global optimum of (30). ■

The final quantizer synthesis therefore has two DP layers: Algorithm 1 is first used to compute the scalar cost curves $\Phi_\ell(N)$ for candidate level counts, after which Proposition 2 allocates the total budget across channels. Finally, Algorithm 1 returns the thresholds and centroids for the selected N_ℓ.

V. Academic Example and Comparative Analysis

We consider an open-loop unstable second-order system (1), described by $A = \left(\begin{smallmatrix} 1.2 & 0.4 \\ -0.3 & 0.9 \end{smallmatrix}\right)$, $B = (1\ 0.5)^\top$, $C = (1\ 1)$, with sampling period $\tau = 0.1$. The LQI controller is designed using $Q = \text{diag}([8, 1, 16])$, $R = 1$, with augmented state $z_k \in \mathbb{R}$, leading to $K = (-1.3755, 0.0368, -1.1107)$ in (7), with a settling time $t_s \approx 12.6$ $[s]$. For illustration, suppose that the application requires a reference trajectory composed of three parts: a constant step $r(t) = -0.7$ for $t \in [0, 40]$ $[s]$, a ramp transition with slope $3{\times}10^{-2}$, for $t \in [40, 80]$ $[s]$, ending at $r(80) = 0.5$, to which a sine trajectory $r(t) = 0.5 {+} 0.3 \sin(2\pi 0.005 t + \pi)$ is then applied for $t \in [80, 160]$ $[s]$. The mixed step-ramp-sine reference emulates prescribed setpoint profiles common in industrial thermal processing and planned tracking trajectories in robotics [13]. Temperature sensors are often networked, leading to the practical setup outlined in the letter, tailored to closed-loop tracking performance.

The data-driven experiment comprises 500 trajectories for training and 250 trajectories for validation, with $\gamma = 0.9992$. Initial conditions are sampled from $x_0 \in [-5, 5]^2$, $z_0 \in [-1, 1]$. To enlarge the operating set, the training and validation references are regularized by bounded multiplicative perturbations of at most 50%, leading to $\bar{r} = 1.2$ in Assumption 2. Using the sampled operating set and Lemma 1, we certify the quantizer domains $(X_1, X_2, Y_1) = (9.15, 15.79, 17.15)$ in (4).

Considering $Q_\delta = Q \succ 0$ in (20), alongside weights (21), we obtain $(\alpha_{x,1}, \alpha_{x,2}, \alpha_{y,1}) = (25.18, 0.67, 7.50)$ in (26). We use a fixed total level budget $N_{\text{total}} = 384$, equivalent to 7 bits per channel on average, with $N_{\min} = 16$. To assess the allocation layer from Proposition 2, we compare four allocations across (x_1, x_2, y): the proposed *performance-aware* allocation (30); a classical *high-rate* allocation $N_\ell \propto (\alpha_\ell S_\ell^2)^{1/3}$; a *signal-only* allocation obtained from the DP allocation with the sensitivity factors α_ℓ removed from (28); and an *equal allocation*. Algorithm 1, combined with (30), gives the proposed quantizer design $(N_{x,1}^\star, N_{x,2}^\star, N_y^\star) = (201, 77, 106)$. Table I isolates the effect of the level-allocation rule using DP scalar quantizers throughout. The proposed allocation provides the least degradation among the above baselines.[1]

Having selected the proposed allocation, we compare scalar quantizer constructions under the same level counts. The baselines are uniform quantization, logarithmic companding μ-law (G.711 codec) $F(\sigma) = \text{sgn}(\sigma) \frac{\ln(1+\mu|\sigma|)}{\ln(1+\mu)}$ on $[-1, 1]$ [20], and locally-optimal Lloyd-Max quantization [21] fitted on the

[1]The source code and full-precision results are available at: https://github.com/mirceasusca/lcss-2026-quantization

Allocation	$(N_{x,1}, N_{x,2}, N_y)$	mean J_γ (18)	mean $\mathcal{S}_\gamma$ (20)
Proposed	$(201, 77, 106)$	$\mathbf{1.249}$	$\mathbf{1.238}$
High-rate	$(157, 68, 159)$	1.605	1.615
Signal-only	$(129, 156, 99)$	2.677	2.698
Equal-level	$(128, 128, 128)$	2.479	2.503

TABLE I

ALLOCATION SENSITIVITY FOR DP QUANTIZERS UNDER $\boldsymbol{N_{\text{total}} = 384}$.

Method	mean J_γ (18)	std J_γ	mean $\mathcal{S}_\gamma$ (20)	std $\mathcal{S}_\gamma$
Uniform	177.8422	23.6404	83.3794	1.2689
Logarithmic	9.0158	0.7286	8.9300	0.2656
Lloyd-Max	2.1262	0.6090	2.1107	0.4360
Proposed DP	$\mathbf{1.4106}$	$\mathbf{0.2573}$	$\mathbf{1.3997}$	$\mathbf{0.1754}$

TABLE II

QUANTIZER-TYPE COMPARISON USING THE PROPOSED ALLOCATION.

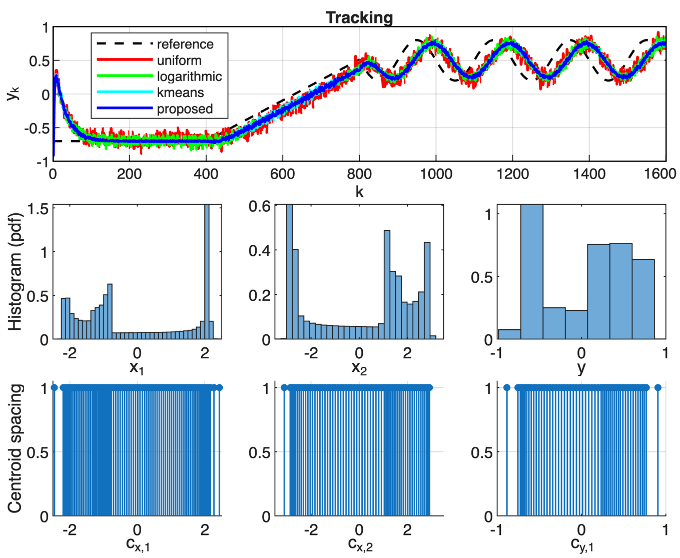

Fig. 2. Tracking response and quantizer correlation to point distribution

same weighted samples. The proposed scalar design uses the globally optimal 1D DP construction of [19]. Table II reports the means and standard deviations of the true discounted cost (18) and surrogate series (20) on the perturbed validation data. The two metrics give the same ordering among the non-uniform designs, and the proposed DP design gives the lowest values.

Lastly, Figure 2 visualizes the proposed design. The top row shows a representative tracking trajectory under the specified reference, where the proposed DP quantizer achieves visibly tighter tracking than the baseline methods, consistent with Table II. The remaining rows pair, for each channel (x_1, x_2, y), the histogram of ideal samples with the corresponding DP centroids. This illustrates how the method combines performance-aware level allocation across channels with non-uniform centroid placement within each channel, with no saturation observed on the validation trajectories.

VI. CONCLUSIONS AND FUTURE WORK

The proposed finite-level quantizer synthesis procedure using accelerated dynamic programming shows reduced closed-loop trajectory distortion compared to relevant counterparts. The method provides a globally-optimal solution to a tractable quadratic surrogate for the desired cost which is tailored to the designed LQI dynamics, with explicit level budget allocation.

Future research directions include: (*i*) incorporating *input* quantization within the same disturbance framework, (*ii*) extending a relevant discounted cost to other control structures, and (*iii*) extending the approach to nonlinear or time-varying dynamics via trajectory-dependent datasets and local models.

REFERENCES

[1] K. Tanaka, Y. Minami, and M. Ishikawa, "Nqlib: A python library for noise-shaping quantizer synthesis," *SoftwareX*, vol. 27, p. 101792, 2024.

[2] X. X. Zheng, W. Liu, X. Lou, S. Vlaski, and T. Y. Al-Naffouri, "Quantitative error feedback for quantization noise reduction of filtering over graphs," *IEEE Transactions on Signal Processing*, pp. 1–16, 2026.

[3] Q. Liu, P. Yu, M. Zapater, and D. Atienza, "Sigmaquant: Hardware–aware heterogeneous quantization method for edge dnn inference," *IEEE Trans. on Circuits and Systems for Artificial Intelligence*, pp. 1–14, 2026.

[4] H. Zou, C. Zhang, S. Lasaulce, L. Saludjian, and H. V. Poor, "Goal-oriented quantization: Analysis, design, and application to resource allocation," *IEEE Journal on Selected Areas in Communications*, vol. 41, no. 1, pp. 42–54, 2022.

[5] R. Brockett and D. Liberzon, "Quantized feedback stabilization of linear systems," *IEEE Trans Aut Control*, vol. 45, no. 7, pp. 1279–1289, 2000.

[6] S. Yüksel and T. Başar, *Stochastic Networked Control Systems: Stabilization and Optimization under Information Constraints*. Birkhäuser New York, NY, 2013.

[7] J. E. Rodriguez Ramirez, Y. Minami, and K. Sugimoto, "Synthesis of event-triggered dynamic quantizers for networked control systems," *Expert Systems with Applications*, vol. 109, pp. 188–194, 2018.

[8] M. Di Ferdinando, S. Di Gennaro, D. Bianchi, and P. Pepe, "On robust quantized sampled-data tracking control of nonlinear systems," *IEEE Trans. on Automatic Control*, vol. 69, no. 10, pp. 7120–7127, 2024.

[9] M. Şuşcă, V. Mihaly, Z. Lendek, I.-C. Morărescu, and P. Dobra, "Controller redesign to minimize uniform quantization errors in uncertain linear systems with fixed hardware constraints," *Nonlinear Analysis: Hybrid Systems*, vol. 60, p. 101683, 2026.

[10] D. Souza, V. de Mesquita, L. Reis, W. Silva, and J. Batista, "Optimal lqi and pid synthesis for speed control of switched reluctance motor using metaheuristic techniques," *Int. J. Control Autom. Syst.*, vol. 19, p. 221–229, 2021.

[11] G. Prestes, F. P. Scalcon, C. Filho, G. Fang, and R. Vieira, "Optimized discrete-time lqi current control for indirect torque regulation of switched reluctance motors," *IEEE Trans. Power Electron.*, pp. 1–13, 2026.

[12] J. Jiao, H. L. Trentelman, and M. K. Camlibel, "Distributed linear quadratic optimal control: Compute locally and act globally," *IEEE Control Systems Letters*, vol. 4, no. 1, pp. 67–72, 2020.

[13] Y. Fang, C. Gu, Y. Zhao, W. Wang, and X. Guan, "Smooth trajectory generation for industrial machines and robots based on high-order s-curve profiles," *Mechanism and Machine Theory*, vol. 201, p. 105747, 2024.

[14] K. Echigo, C. R. Hayner, A. Mittal, S. B. Sarsılmaz, M. W. Harris, and B. Açıkmeşe, "Linear programming approach to relative-orbit control with element-wise quantized control," *IEEE Control Systems Letters*, vol. 7, pp. 3042–3047, 2023.

[15] X. Wang, L. Li, M. Shen, X. Zhao, Q.-G. Wang, and Z. H. Zhu, "Data identification optimal control for quantized linear systems under dos attacks," *IEEE Transactions on Aerospace and Electronic Systems*, vol. 61, no. 4, pp. 10 874–10 881, 2025.

[16] L. Liu, Y. Kawano, and M. Cao, "Design of stochastic quantizers for privacy-preserving control," *IEEE Transactions on Automatic Control*, vol. 71, no. 2, pp. 1160–1174, 2026.

[17] S. Lang and F. Allgöwer, "Minimum data-rate for generalized h2-performance," in *2025 IEEE 64th Conference on Decision and Control (CDC)*, 2025, pp. 547–554.

[18] J. de Brusse, J. Daafouz, M. Granzotto, R. Postoyan, and D. Nešić, "Discounted lqr: stabilizing (near-)optimal state-feedback laws," in *2025 IEEE 64th Conf. on Decision and Control (CDC)*, 2025, pp. 4714–4719.

[19] H. Wang and M. Song, "Ckmeans.1d.dp: Optimal k-means clustering in one dimension by dynamic programming," *R Jrn., 3(2)*, p. 29–33, 2011.

[20] S. W. Smith, *The Scientist and Engineer's Guide to Digital Signal Processing*. California Technical Publishing, 1999.

[21] A. Gersho and R. Gray, *Vector Quantization and Signal Compression*. Springer (SECS, volume 159), 1992.